The Influence of the Substitution Pattern on the Molecular Conformation of Ureido-1,2,5-oxadiazoles, Related to STAT3 Inhibitors: Chemical Behavior and Structural Investigation

by **Stefania Villa**, **Daniela Masciocchi**, **Arianna Gelain**, and **Fiorella Meneghetti***

Department of Pharmaceutical Sciences 'Pietro Pratesi', University of Milan, via L. Mangiagalli 25, IT-20133 Milano
(phone: +39-02-503-19306; fax: +39-02-503-19359; e-mail: fiorella.meneghetti@unimi.it)

Signal transducer and activator of transcription 3 (STAT3) is a protein constitutively activated by aberrant upstream tyrosine kinase activities in a broad spectrum of human solid and blood tumors. Therefore, the availability of drugs affecting STAT3 may have important therapeutic potential for the treatment of cancer. Pursuing our efforts in exploring the influence of the substitution pattern of the ureido 1,2,5-oxadiazole moiety on the molecular conformation, new compounds substituted at positions 3 and 4 on the furazane ring were synthesized. The inhibition properties *vs.* STAT3 of the novel compounds were evaluated in a dual-luciferase assay, using HCT-116 cells, and the results evidenced a moderate activity only for the compounds endowed with a planar arrangement. Crystallographic studies of the new derivatives were performed in order to evidence the peculiar chemical behavior and to evaluate how structural modulations affected the biological properties.

1. Introduction. – Signal transducer and activator for transcription 3 (STAT3) is a latent cytosolic protein that directly relates extracellular signals (growth factors, polypeptide, cytokines, *etc.*) from the membrane to the nucleus. STAT3 Proteins constitute an important point of convergence for many signaling pathways that are commonly activated in cancer cells. Binding of growth factors or cytokines to their receptors results in the activation of intrinsic receptor tyrosine-kinase activity or receptor-associated kinases, such as the *Janus* kinase (JAK) or Src tyrosine kinases. These enzymes subsequently phosphorylate the cytoplasmic tails of the receptor to provide the docking sites for the recruitment of monomeric STAT3, then STAT3s themselves become substrates for tyrosine phosphorylation. Non-receptor tyrosine kinases, such as the oncoproteins Src and Bcr-Abl (a fusion of the breakpoint-cluster region (Bcr) and *Abelson* leukaemia (Abl) proteins), can phosphorylate STAT3 independently of receptor engagement. Phosphorylated STAT3 dimerizes and translocates to the nucleus, where the dimers directly regulate gene expression. Whereas STAT3 activation is tightly regulated in normal cells, the persistent activation of tyrosine kinases in cancer causes constitutive activation of STAT3 [1–9]. This leads to permanent changes in the expression of genes controlling fundamental cellular processes, which are subverted in cancer cells. STAT3 is constitutively activated by aberrant upstream tyrosine kinase activities in a broad spectrum of human solid tumors, including breast, brain, colon, prostate, lung, pancreatic, pituitary, gastrointestinal, ovarian, cervical tumors, and melanoma, as well as hematological malignancies such as

lymphomas and leukemias [10][11]. Since STAT3 inhibition leads to apoptosis in tumor cells, but not in normal cells [12][13], it represents a promising target for therapeutic intervention. At present, there is no report of an approved drug targeting STAT3, even though a number of small molecules were discovered as potential STAT3 inhibitors [14].

An attempt to find inhibitors of this pathway, by the known dual-luciferase assay system with cancer cell line harboring abnormally activated STAT3, the ureido-oxadiazole derivative AVS-0288 (**I**) was disclosed as potential anticancer agent, due to its ability to significantly decrease STAT3 activity [15]. To build up a validated pharmacophoric model and to understand the bases for its STAT3 inhibitory activity, we investigated the effects of a series of modifications structurally related to **I**. In particular, we studied the effects of the chlorophenyl replacement to C(4) of the heterocycle and simultaneously the insertion of a CH_2 group between the ureido and the *N*-phenyl moieties. The previous biological data revealed that, of the ureido series, several derivatives showed interesting results [16]. The structure–activity relationships study (SAR) on these compounds highlighted that a polar substituent at C(4) had detrimental effect on the activity, while the insertion of the benzylic side chain linked to the ureido moiety was tolerated (compound **1a**, R = CH_2OH). Starting from this point, we investigated the molecular modifications of the substitution at C(4), synthesizing two derivatives, **2a** (R = CHO) and **3a** (R = Me), related to **1a**. They bear a substituent selected to fine-tune the influence on the activity of lower-polarity groups, to establish whether the presence of an aromatic moiety at C(4) is essential to confer the STAT3 inhibitory activity. The syntheses of **2a** and **3a** revealed significant differences in their chemical behaviors compared to the previously reported oxadiazole derivatives [16]. The earlier studies indicated that an extended molecular conformation was critical for the activity; we now suggest that the loss of the inhibitory potency of a number of ureido derivatives could be mainly due to conformational changes that interfered at the STAT3 binding site. Therefore, we synthesized the isomers (*E*)- and (*Z*)-**4a** (R = PhCH=CH), which bear a benzyl (Bn) chain linked to the ureido moiety. The choice of the styryl group was considered to clarify the molecular requirements at C(4), by selecting a group able to confer a planar molecular conformation. Then, we prepared the styryl derivatives (*E*)- and (*Z*)-**4b** with a Ph ring directly linked to the ureido moiety, as in **I**, to evaluate if the conjugation effect along the entire molecule is required for the extended conformation of the compounds. Taking into account the similarity in the chemical structure among the active compound **I** and the considered derivatives, little changes in functional groups were analyzed, in order to understand the SAR associated to the flexibility of the ureido moiety, as it seems to play an important role for the observed biological activity.

In this article, we describe the syntheses of **1a** and **1b**, **2a** and **2b**, **3a**, (*E*)-**4a** and (*E*)-**4b**, and (*Z*)-**4a** and (*Z*)-**4b**, highlighting the most interesting aspects of the reaction paths, together with the investigation of their molecular conformation by means of X-ray analysis, and then their biological data will be compared with the those of reference compound.

2. Results and Discussion. – 2.1. *Chemistry.* The syntheses of compounds **1a** and **1b** and **2a** and **2b** were performed starting from **6**, which was prepared according to the

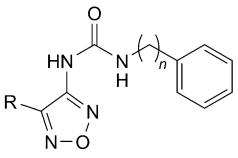

	n	R
1a	1	HO–CH_2
1b	0	HO–CH_2
2a	1	CHO
2b	0	CHO
3a	1	Me
(*E*)-**4a**	1	PhCH=CH
(*Z*)-**4a**	1	PhCH=CH
(*E*)-**4b**	0	PhCH=CH
(*Z*)-**4b**	0	PhCH=CH

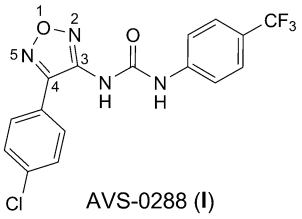

AVS-0288 (**I**)

procedure described in [16]. The general synthetic approach, used to introduce the planned functional groups in the oxadiazole ring, involved a condensation reaction between the NH_2 group of the key intermediates 3-amino-1,2,5-oxadiazoles, differently substituted at C(4), and benzyl or phenyl isocyanate (BnNCO and PhNCO, resp.) under microwave (MW) irradiation. For the synthesis of **1a** and **1b**, before the condensation, the alcohol function was protected by ClCOOMe. The MW-assisted reactions were necessary to obtain the designed compounds, as the conventional conditions were not efficient. The toluene solutions of **7** and the corresponding isocyanate in equimolar amounts were irradiated to obtain the expected ureido derivatives **8a** and **8b**, selecting time and temperatures in order to optimize the yields (*Scheme 1*). The OH group was then deprotected and oxidized with *Dess–Martin* periodinane in dry CH_2Cl_2 to give the corresponding aldehydes **2a** and **2b**. In solution, compounds **2a** and **2b** underwent spontaneous cyclization to form **5a** and **5b**, respectively obtained through the intramolecular reaction between the ureido N-atom and the aldehyde function. This is in agreement with the intramolecular ring closures

Scheme 1. *Synthesis of Compounds* **1a** *and* **1b** *and* **2a** *and* **2b**

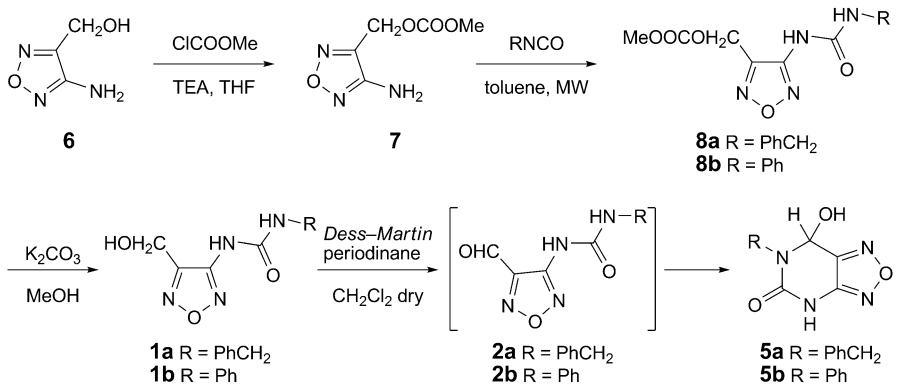

when aldehydes bind to N-atoms able to give hemi-aminals inside the stable medium-sized rings [17–23]. It was not possible to follow the cyclization reaction by NMR, as the equilibrium was completely shifted towards the cyclic form. Compounds **5a** and **5b** were the only products isolated as established by ^{1}H-NMR spectroscopy. The following single-crystal X-ray analysis on **5a** supported unambiguously the proposed structure. By the same methodology [16] for preparing compound **3a**, we detected an anomalous reactivity of the precursor **9** during the reaction with BnNCO in toluene under MW irradiations (*Scheme 2*). After cooling a solid fraction precipitated from the reaction mixture, TLC analysis revealed the presence of one product, **3a**, in the solution, while in the solid fraction other two compounds, **10** and **11**, were identified. Suitable crystals for X-ray analysis of the two different portions were obtained, and the crystallographic results confirmed that the toluene-soluble product was the expected **3a**, while the solid material was constituted by two not separable symmetrically disubstituted ureas **10** and **11** (see *Scheme 2* and *Crystallographic Studies*). The formation of the *N*,*N*′-dibenzylurea (**11**) is an expected side-product formed in presence of trace of H_2O by nucleophilic addition to the isocyanate C-atom [24]. On the contrary, the other compound, **10**, was an unusual product (to the best of our knowledge, only one patent in the literature [25]), and its formation can be rationalized as outlined in *Scheme 3*. The starting amine **9** reacted with BnNCO to give the desired ureido derivative **3a**. A thermal conversion of **3a** led to the formation of the corresponding isocyanate, which instantly reacted with the initial amine **9** in excess to form the symmetrically substituted urea **10**. As continuation of our work, we investigated, in this series of compounds, the influence of

Scheme 2. *Synthesis of Compound* **3a**

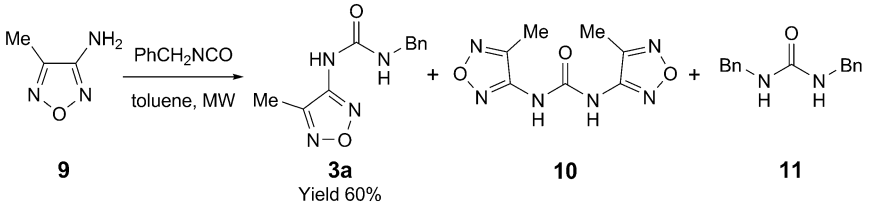

Scheme 3. *Proposed Mechanistic Pathway for the Formation of Compound* **10**

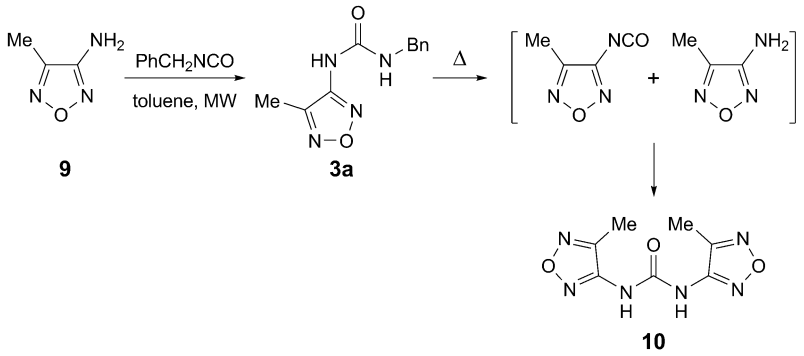

an aromatic group at C(4) on both the activity and the conformation. Since the urea linkage plays an active role in the solid-state conformation, and it governs the overall shape of the molecules, the introduction at C(4), of a vinyl spacer, bearing a Ph group, allowed us to verify if the resonance effect between the oxadiazole and the substituent at C(4) is determinant for the *trans*/*trans*-conformation of the ureido moiety. We synthesized compounds with the styryl moiety at C(4) by exploiting the aldehydic reactivity of the cyclic hemiaminals **5a** and **5b** [26]. The products (*E*)-**4a** and (*Z*)-**4a** and (*E*)-**4b** and (*Z*)-**4b** were obtained by a *Wittig* reaction between **5a** and **5b**, respectively, and Bn(Ph_3)PCl under basic condition in THF at reflux, as *ca.* 3:1 (*E*)/(*Z*) mixtures (*Scheme 4*). The (*E*)-and (*Z*)-isomers were easily separated by silica-gel chromatography. The assignment of the (*E*)/(*Z*) geometry about the styryl π-bond was achieved by H,H- coupling constants for the olefinic H-atom signals and confirmed by X-ray analysis.

Scheme 4. *Synthesis of compounds* (*E*)-**4a** *and* (*E*)-**4b** *and* (*Z*)-**4a** *and* (*Z*)-**4b**

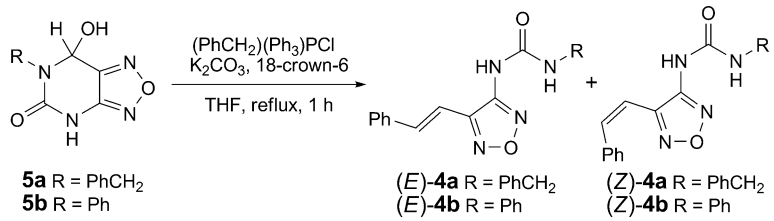

2.2. *Biology.* The biological data showed that compounds **3** and **5** were inactive, while the two styryl isomers (*E*)-**4a** and (*Z*)-**4a** exhibited inhibitory activity of 15.71 and 21.20%, respectively (*Table 1*). In particular, (*E*)- and (*Z*)-**4a** exhibited inhibitory

Table 1. *STAT3 Inhibitory Activity of Compounds* **3**–**5** *by Dual-Luciferase Assay*

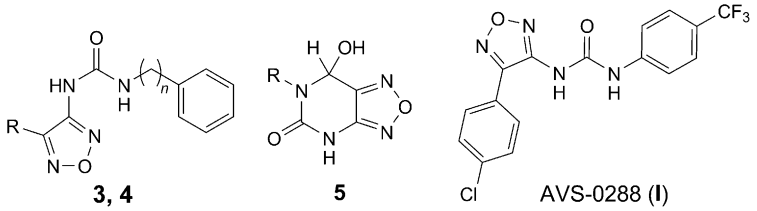

Compounds	*n*	R	Inhibition[a]) at 2 μM [%]
3a	1	Me	<1
(*E*)-**4a**	1	PhCH=CH	15.71
(*Z*)-**4a**	1	PhCH=CH	21.20
(*E*)-**4b**	0	PhCH=CH	<1
(*Z*)-**4b**	0	PhCH=CH	<1
5a	–	$PhCH_2$	<1
5b	–	Ph	<1
AVS-0288 (**I**)	–	–	45.00

[a]) The values are means of three experiments and the maximum deviation was less than 10%.

activities comparable to several 4-phenyl-substituted derivatives [16], to support the hypothesis concerning the important presence of an aromatic group at C(4). Isomers (*E*)- and (*Z*)-**4a** retained a modest activity probably due to the electronic conjugation of the styryl chain with the oxadiazole, which favored the establishment of stacking interactions with the biological target. The drop in activity of these derivatives with respect to **I** could be due to the presence of the flexible Bn chain linked to the ureido moiety that disrupted the flat conformation of the molecule. To check if the above hypothesis might have a correspondence in the solid state, isomers (*E*)- and (*Z*)-**4b** with a Ph group linked to the ureido moiety were prepared, and the data obtained for (*E*)- and (*Z*)-**4b** showed the absence of inhibitory activity; therefore, the styryl system is not determinant to guarantee a planar arrangement and at the same time an extended conformation.

2.3. *Crystallographic Studies.* The X-ray molecular structures of the compounds **1a**, **5a**, **3a**, **10**–**11**, (*E*)-**4a**, and (*E*)-**4b** are presented, as ORTEP views [27], in *Fig. 1*.

Compound **1a** presents a *cis*/*trans* arrangement of the two amide bonds due to the formation of the intramolecular H-bond N4–H4···N2; distance, 2.21(1) Å; angle, 130(1)°. The two rings form a dihedral angle of 57(1)°. A three-dimensional network, stabilized by N–H···O H-bonds, Cπ–H···O intermolecular contacts, and aromatic stacking involving the oxadiazole rings, characterizes the molecular assembly. The bicyclic derivative **5a** has a folded conformation, defined by the dihedral angle of 86(1)° between the oxadiazole and Ph moieties. The six-membered ring C1/C2/C3/N3/C11/N4 adopts a half-boat conformation with puckering parameters $Q_T = 0.157(3)$ Å and $\theta_2 = 106.8(9)°$ [28]. The intermolecular H-bonds involve O31–H···O2^{I} (distance 1.63(1) Å, angle 157(1)° (^{I} at $1-x, -y, 1-z$)) and N4–H···O3^{II} (distance, 1.99(1) Å, angle, 176(1)° (^{II} at $x+1, y, z$)), with the formation of cyclic dimers further extended into a two-dimensional network. The molecular packing is consolidated by π–π stacking of the oxadiazole rings (centroid–centroid distance of 3.34(1) Å) and by weak Cπ–H···N contacts: C8–H···N2^{III} (distance, 2.91(1) Å; angle, 131(1)° (^{III} at $x-1, y, z+1$)). In the crystal structure of **3a**, as in **1a**, the formation of the intramolecular H-bond N4–H4···N2, (distance, 2.01(1) Å; angle, 136(1)°) favors the *cis*/*trans* conformation of the ureido moiety. The dihedral angle of 88(1)° between the oxadiazole and the Ph moieties evidences the curled-up shape of the molecule, determined by the different orientations of the two rings. Its crystal packing is characterized by dimers stabilized by N3–H···O2^{I} H-bonds (distance, 1.91(1) Å; angle, 176(1)° (^{I} at $2-x, -y, 1-z$)). In the $C_7H_8N_6O_3 \cdot C_{15}H_{16}N_2O_1$ (**10**–**11**) co-crystals, the two molecules are located on a crystallographic twofold axis coincident with the carboxylic bond. Compound **10** is essentially planar, while **11** is characterized by a 'Z' shape, with the two symmetry-related benzene moieties almost perpendicular to the ureido plane (dihedral angle, 77(1)°), with the dihedral angle of 15(1)° between them. The two different units are connected by two bifurcated H-bonds, the strong N3b–H···O2c^{I} (distance, 1.87(1) Å; angle, 155(1)° (^{I} at $½-y, -, ½-z$)) and the looser one N3c–H···O2b^{II} (distance, 2.19(1) Å; angle, 151(1)° (^{II} at $1-x, 1-y, z$)). The three-dimensional arrangement of the molecules gives rise to the formation of columnar structures along the 4_2 axis of the tetragonal cell. The formation of reciprocal H-bonds between the ureido H-atoms and the C=O O-atoms of **10** and **11** acted as stabilizing factors, giving reason to the separation of the crystalline adduct **10**–**11** from the reaction mixture. Bifurcated H-

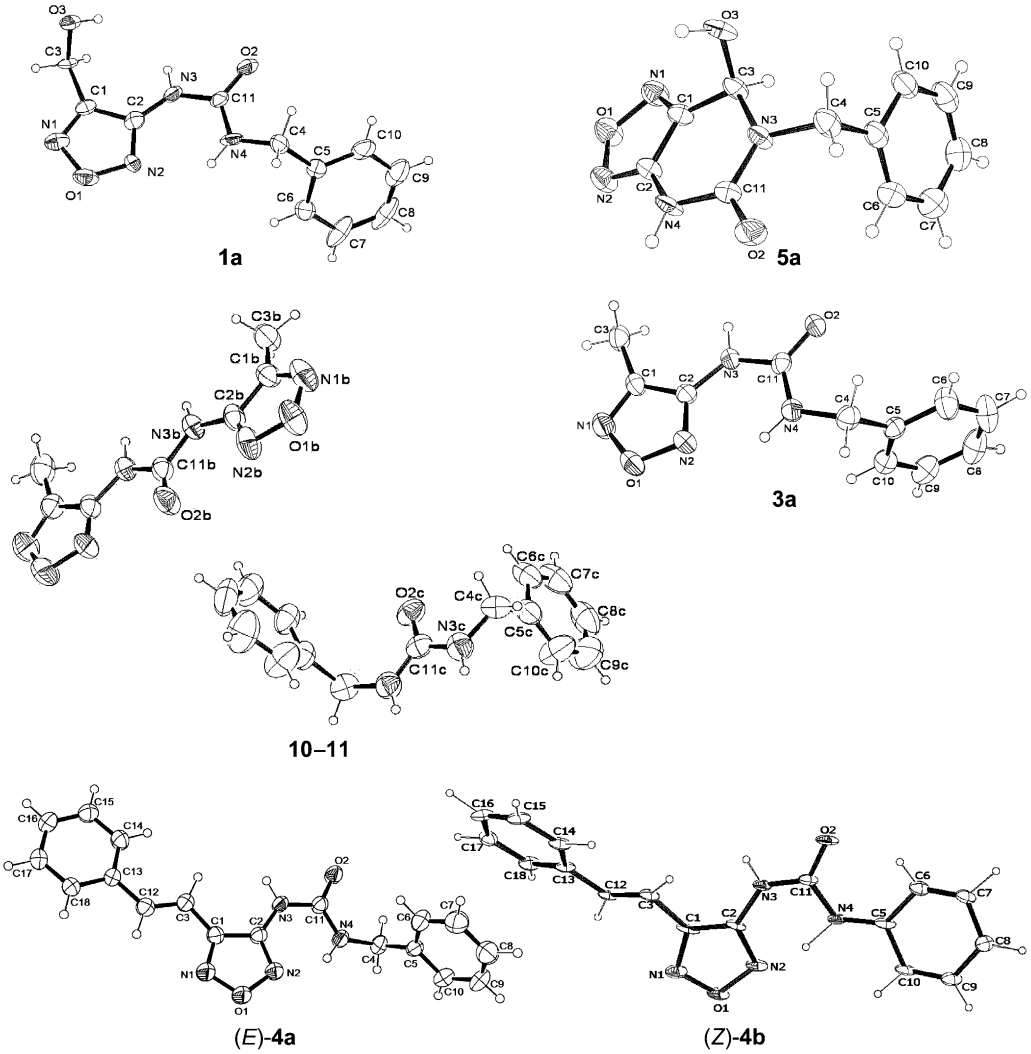

Fig. 1. *ORTEP* [28] *Views of the molecular structures with the relative atom-numbering scheme.* In the adduct **10**–**11**, labeled atoms are related to unlabeled by binary symmetry (thermal ellipsoids at 30% probability).

bonds are a common motif in diaryl-urea and their molecular complexes (*Fig. 2*) [29][30].

The crystal structures of (*E*)-**4a** and (*E*)-**4b** confirmed the (*E*) configuration of the styryl C=C bond. In (*E*)-**4a**, the π-conjugated system is essentially planar with a dihedral angle of 3.3(1)° between the oxadiazole and Ph rings, while the two Ph rings are almost orthogonal with a dihedral angle of 82(1)°. In (*E*)-**4b**, the Ph ring of the styryl moiety is rotated by 53.4(1)° with respect to the heterocyclic ring; that twist disfavors the transmission of the resonance effect along the CPh–C=C–C(het) moiety.

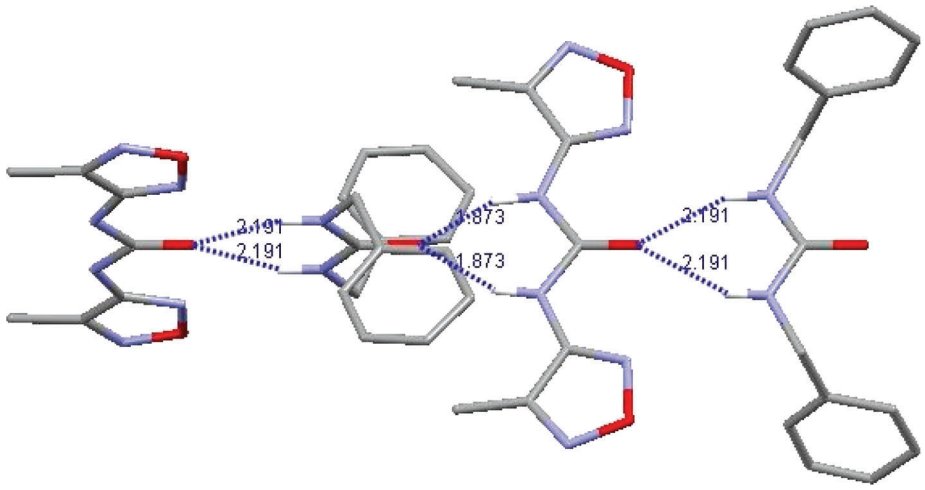

Fig. 2. *Partial packing diagram with the H-bond pattern involving compounds* **10** *and* **11**, *leading to the formation of the chain along the* b *axis* (H-bond distances are reported)

This is revealed by the shorter values of the C12–C13 and C1–C3 bond lengths in (*E*)-**4a** (1.456(4) and 1.44(4) Å *vs.* 1.477(7) and 1.501(7) Å for (*E*)-**4a** and (*E*)-**4b**, resp.), characterized by a higher coplanarity between the two rings. In (*E*)-**4b**, the Ph group linked to the ureido moiety is almost coplanar with the oxadiazole, having a dihedral angle of 14(1)°, while the two Ph rings are rotated by 53.0(1)°. In both compounds, the intramolecular H-bond N4–H···N3 is present, so the ureido group adopts a *cis*/*trans*-conformation at the two amide bonds. In (*E*)-**4a**, the N4–H···N3 H-bond is characterized by a distance of 1.93(1) Å and an angle of 143(1)°, in (*E*)-**4b**, the same atoms are engaged in a stronger interaction, as shown by the value of the distance of 1.54(6) Å and of an angle of 160(1)°. The *cis*/*trans* ureido conformation in (*E*)-**4b** is further stabilized by the intramolecolar contact C6–H···O2 of 2.13(1) Å and an angle of 140(1)°. The existence of this intramolecular interaction between the aromatic H-atoms of the Ph ring with the ureido O-atom is a key feature which imparts additional stability to the molecular conformation in the solid state. In the crystal, molecules of (*E*)-**4a** and (*E*)-**4b** are arranged in a similar manner. The crystal packing is built up by centrosymmetric dimers joined by N3–H···O2^{I} H-bonds. Weak contacts link adjacent dimers, type Cπ–H···O and Cπ–H···N in (*E*)-**4a** and (*E*)-**4b**, respectively, leading to the formation of infinite chains. In the crystal of (*E*)-**4a**, π–π interactions are also present between nearly parallel oxadiazole and styryl moieties of neighboring molecules stacked along the *c* axis in a head-to-tail manner (centroid-to-centroid distance of 4.1(1) Å).

As demonstrated by the crystallographic results (*Fig. 3*), all derivatives, **1a**, **3a**, (*E*)-**4a**, and (*E*)-**4b**, are characterized by a constrained conformation, resulting from the rotation of the ureido moiety, due to the formation of a $N_{het}H\cdots N_{urea}$ intramolecular H-bond, differently to **I**.

In the crystal structure of **I** [16], we found that the two ureido H-atoms are not involved in intramolecular contacts, thus they could participate in H-bonds at the

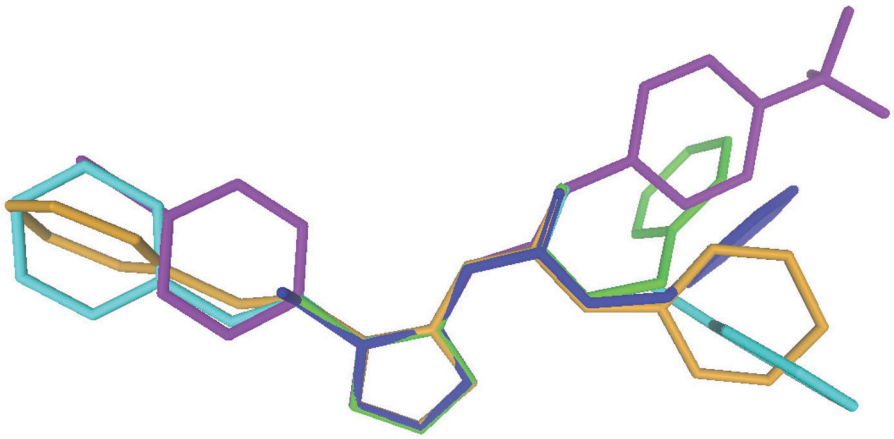

Fig. 3. *Superimposition of the crystal structures of* **I** (violet), **1a** (blue), **3a** (green), *and* (E)-**4a** (light blue) *and* (E)-**4b** (orange) *achieved by overlaying the oxadiazole rings.* H-Atoms are omitted for clarity.

macromolecular binding site. In addition, its flat conformation could favor the π-interactions with the aromatic residue present in the binding pocket. Beside that, the pendant halogen atoms play a very important role in anchoring **I** in the binding site in extended conformation, so to prevent in this way the formation of the $N_{het}H\cdots N_{urea}$ interaction. On the basis of these findings, we can assume that the binding mode of the ureido derivatives related to **I** requires that the oxadiazole–ureido group adopts an extended orientation. This could be provided by positive hydrophobic interactions at the active site, thus validating the Ph rings as anchor for hydrophobic arms capable to interact with the target. This hypothesis is supported by the presence of a intermolecular interaction network in the crystal structure of **I** involving the halogen atoms, implicated in keeping a flat molecular conformation. Further, the lipophilicity of these moieties can modulate in a suitable way the absorption properties of the molecule, as they can find in the hydrophobic side chains, present in the binding site, a favorable environment. In this respect, it is important to underline that C–F$\cdots$H–C type interactions were reported to play an important role in crystal packing and in the biological systems [31]. This suggests that different contacts of the hydrophobic part of the molecule may guide the H-bonding interaction pattern of the ureido moiety, and the overall molecular conformation in the bound and unbound forms.

3. Conclusions. – The present work highlights that the biological inactivity of **1a** and **3a** could be explained as they lack both of the key requirements previously indicated: an aromatic moiety at C(4) and the extended conformation. Besides, the introduction of a styryl moiety led to a moderate STAT3 inhibition in isomers (*E*)- and (*Z*)-**4a**. Nevertheless, (*E*)- and (*Z*)-**4b** lost the inhibitory properties, indicating that the styryl chain could not always place the Ph ring in a suitable orientation inside the binding pocket, and the resonance effect was not determinant to guarantee an extended conformation and a planar arrangement. The crystal structure of (*E*)-**4b** showed that the substitution of the flexible Bn chain linked to the ureido moiety with a Ph ring did

not thoroughly influence the *trans*/*trans*-arrangement of the ureido bond. Indeed, in this compound, the folded conformation could be also stabilized by an additional Cπ–H$\cdots$O intramolecular interaction. From the SAR point of view, we propose the important role played at the binding site of the halogen atoms, present in the reference compound **I**, in keeping the extended conformation, implying that the substitution pattern on both phenyl rings should be taken into account as a critical factor. In **I**, the intermolecular contacts of the CF_3 group could prevent the formation of the intramolecular $N_{het}H\cdots N_{urea}$ H-bond, so the two N–H donors and the C=O acceptors of the ureido moiety remained available for guest binding.

In summary, the detailed solid-state investigation of these derivatives provided useful insight on the different factors contributing to the pre-organization of the variable conformations of the ureido-oxadiazole group, supporting the hypothesis that conformational changes have a strong effect on the STAT3 inhibitory properties, and affording new information for further lead optimization of this class of compounds.

Experimental Part

1. *General*. Reagents were purchased from *Sigma–Aldrich* and were used without any further purification. Compounds **6** and **9** were synthesized according to literature methods [16][32]. The reactions were performed under conventional conditions or by microwave (MW) irradiation (*Biotage-Initiator.2*). Reactions were monitored by TLC on aluminium-backed *Merck* Silica Gel *60* plates (0.2 mm). Intermediates and final compounds were purified by flash chromatography using *Merck* silica gel *60* (70–230 mesh). The purity of final compounds was determined by HPLC analysis and were $\geq$ 95%. M.p.: in open cap. tubes on a *Büchi Melting Point B-540* apparatus. ^{1}H-NMR Spectra: at r.t., *Varian 300* MHz *Oxford* instrument, chemical shifts (δ) in ppm from TMS resonance in the indicated solvent (TMS: 0.0 ppm). All new compounds gave satisfactory C, H, N elemental analyses ($\pm$0.4%).

2.1. *Synthesis of (4-Amino-1,2,5-oxadiazol-3-yl)methyl Methyl Carbonate* (**7**). Compound **7** was synthesized according to the procedure reported in [16].

2.2. *General Procedure for the Synthesis of Methyl (4-Ureido-1,2,5-oxadiazol-3-yl)methyl Carbonate Derivatives* **8a** *and* **8b**. A mixture of **7** (50 mg, 0.29 mmol) and the appropriate isocyanate (0.40 mmol, 0.05 ml) in toluene (1 ml), in a sealed vial, was irradiated in a MW synthesizer at 300-W at a temp. of 180° for 40 min. After cooling, a white jelly-like solid began to precipitate. The solid was filtered and washed with toluene.

[4-(3-Benzylureido)-1,2,5-oxadiazol-3-yl]methyl Methyl Carbonate (=*{4-[(Benzylcarbamoyl)-amino]-1,2,5-oxadiazol-3-yl}methyl Methyl Carbonate*; **8a**). Yield: 31%. ^{1}H-NMR ($CDCl_3$): 3.80 (*s*, MeO); 4.60 (*d*, *J* = 5.7, CH_2); 5.35 (*s*, CH_2O); 7.25–7.35 (*m*, 5 arom. H); 8.60 (*s*, NH, exchangeable with D_2O).

[4-(3-Phenylureido)-1,2,5-oxadiazol-3-yl]methyl Methyl Carbonate (= *Methyl {4-[(Phenylcarbamoyl)amino]-1,2,5-oxadiazol-3-yl}methyl Carbonate*; **8b**). Yield: 35%. ^{1}H-NMR ($CDCl_3$): 3.80 (*s*, MeO); 5.40 (*s*, CH_2O); 7.20–7.60 (*m*, 5 arom. H); 8.60 (*s*, NH, exchangeable with D_2O); 9.20 (*s*, NH, exchangeable with D_2O).

2.3. *General Procedure for the Synthesis of 1-Aryl-3-[4-(Hydroxymethyl)-1,2,5-oxadiazol-3-yl]urea Derivatives* **1a** *and* **1b**. Compound **8a** and **8b** (50 mg, 0.16 mmol), resp., was dissolved in 1% soln. of K_2CO_3 in MeOH (2 ml), and the resulting soln. was stirred at reflux for 2 h. After completion of the reaction, MeOH was removed *in vacuo*. The residue was diluted with AcOEt (3 ml) and washed with H_2O (2 $\times$ 1 ml). The org. phase was dried (Na_2SO_4) and evaporated to obtain the white solid.

1-Benzyl-3-[4-(hydroxymethyl)-1,2,5-oxadiazol-3-yl]urea (**1a**). Quant. yield. ^{1}H-NMR ($CDCl_3$): 4.55 (*d*, *J* = 5.7, CH_2); 4.80 (*s*, CH_2); 7.25–7.40 (*m*, 5 arom. H); 8.10 (*s*, NH, exchangeable with D_2O); 10.30 (*s*, NH, exchangeable with D_2O).

1-[4-(Hydroxymethyl)-1,2,5-oxadiazol-3-yl]-3-phenylurea (**1b**). Quant. yield. ^{1}H-NMR (CD_3OD): 4.85 (*s*, CH_2); 7.10–7.50 (*m*, 5 arom. H).

2.4. *General Procedure for the Synthesis of 7-Hydroxy-6,7-dihydro[1,2,5]oxadiazolo[3,4-*d*]pyrimidin-5(4*H*)-one Derivatives* **5a** *and* **5b**. To an ice-cold soln. of the compound **1a** and **1b** (50 mg, 0.20 mmol), resp., in dry CH_2Cl_2 (1.5 ml), *Dess–Martin* periodinane (131.5 mg, 0.31 mmol) was added in one portion. The mixture was stirred at 0° for 30 min and then at r.t. for 24 h. The reaction was quenched at 0° by stirring with a sat. aq. solns. of $Na_2S_2O_3$ (1 ml) and of $NaHCO_3$ (1 ml) for 10 min, to destroy any unreacted *Dess–Martin* reagent. The org. phase was then separated, dried (Na_2SO_4), and concentrated *in vacuo*. The crude product was purified by flash chromatography (petroleum ether (PE)/AcOEt 6:4) to give the cyclic hemiaminals **5a** and **5b** as light yellow powders.

*6-Benzyl-6,7-dihydro-7-hydroxy[1,2,5]oxadiazolo[3,4-*d*]pyrimidin-5(4*H*)-one* (**5a**). Yield: 85%. Light-yellow powder. M.p. 194–196°. ^{1}H-NMR (DMSO): 4.40 (*d*, *J* = 15, CH_2); 4.90 (*d*, *J* = 15, CH_2); 6.10 (*d*, *J* = 9, CH, collapses to a *s* on D_2O exchange); 7.20–7.30 (*m*, 5 arom. H); 7.40 (*d*, *J* = 9, OH, exchangeable with D_2O); 11.3 (*s*, NH, exchangeable with D_2O). ^{13}C-NMR (DMSO): 40.8 (CH_2); 70.4 (OH); 120.8 (arom. CH); 120.9 (2 arom. CH); 120.9 (2 arom. CH); 130.8 (C); 140.4 (arom. C); 150.1 (C); 150.1 (C=O).

*6,7-Dihydro-7-hydroxy-6-phenyl[1,2,5]oxadiazolo[3,4-*d*]pyrimidin-5(4*H*)-one* (**5b**). Yield: 80%. Light-yellow powder. M.p. 182–184°. ^{1}H-NMR ($CDCl_3$): 6.35 (*d*, *J* = 8.7, CH, collapses to a *s* on D_2O exchange); 7.30–7.50 (*m*, 5 arom. H); 7.55 (*d*, *J* = 8.7, OH, exchangeable with D_2O); 11.40 (*s*, NH, exchangeable with D_2O).

Synthesis of 1-Benzyl-3-(4-methyl-1,2,5-oxadiazol-3-yl)urea (**3a**)*, 1,3-Bis(4-methyl-1,2,5-oxadiazol-3-yl)urea* (**10**)*, and 1,3-Dibenzylurea* (**11**). To a soln. of *4-methyl-1,2,5-oxadiazol-3-amine* (**9**; 50 mg, 0.50 mmol) in toluene (1.5 ml), BnNCO (0.60 mmol, 0.08 ml) was added at r.t. The mixture was irradiated in MW synthesizer at 300 W at 170° for 20 min. After cooling, a white solid was collected by filtration and washed with toluene. This solid was an adduct of **10** and **11** (yield 40%, molar ratio 1:1). The remaining mixture was evaporated *in vacuo* and the crude residue was chromatographed on SiO_2 (PE/AcOEt 8:2) to give **3a** (70 mg, 60%). White solid. M.p. 197–199°. ^{1}H-NMR of **3a**: ($CDCl_3$) 2.35 (*s*, Me); 4.55 (*d*, *J* = 5.7, CH_2); 7.20–7.40 (*m*, 5 arom. H); 7.90 (br. *s*, NH, exchangeable with D_2O); 9.90 (br. *s*, NH, exchangeable with D_2O). The adduct **10**–**11** was characterized by X-ray analysis.

2.5. *General Procedure for the Synthesis of 3-(4-styryl-1,2,5-oxadiazol-3-yl)urea Derivatives (*E*)- and (*Z*)-***4a***, and (*E*)- and (*Z*)-***4b***.* A mixture **5a** and **5b** (50 mg, 0.20 mmol), resp., $Bn(Ph_3)PCl$ (90.4 mg, 0.23 mmol), K_2CO_3 (31.8 mg, 0.43 mmol), 18-crown-6 (cat. quantity), and THF (2 ml) as a solvent was stirred at reflux for 1 h. The solvent was evaporated *in vacuo*, and the residue was treated with brine and extracted with AcOEt (3 × 1 ml). The org. layer was evaporated *in vacuo*, and the crude product was purified by flash chromatography (PE/AcOEt 7:3).

*1-Benzyl-3-{4-[(*E*)- and (*Z*)-2-phenylethenyl]-1,2,5-oxadiazol-3-yl}urea* ((*E*) and (*Z*)-**4a**). Yield: 50% of (*E*)-**4a** as a pale yellow solid (m.p. 192–194°) and 19% of (*Z*)-**4a** as a yellow solid (m.p. 170–172°).

*Data of (*E*)-***4a***.* ^{1}H-NMR ($CDCl_3$): 4.59 (*d*, *J* = 5.7, CH_2); 7.20 (*d*, *J* = 15.5, CH); 7.20–7.67 (*m*, 10 arom. H); 7.60 (*d*, *J* = 15.5, CH); 7.98 (*t*, *J* = 5.7, NH, exchangeable with D_2O); 9.96 (br. *s*, NH, exchangeable with D_2O);

*Data of (*Z*)-***4a***.* ^{1}H-NMR ($CDCl_3$): 4.48 (*d*, *J* = 5.7, CH_2); 6.44 (*d*, *J* = 12.2, CH); 7.11 (*d*, *J* = 12.2, CH); 7.20–7.40 (*m*, 10 arom. H); 7.58 (*t*, *J* = 5.7, NH, exchangeable with D_2O); 9.60 (*s*, NH, exchangeable with D_2O).

*1-Phenyl-3-{4-[(*E*)- and (*Z*)-2-phenylethenyl]-1,2,5-oxadiazol-3-yl}urea* ((*E*) and (*Z*)-**4b**). Yield: 55% of (*E*)-**4b** as a yellow solid (m.p. 201–203°) and 25% of (*Z*)-**4b** as a yellow solid (m.p. 173–175°).

*Data of (*E*)-***4b***.* ^{1}H-NMR ($CDCl_3$): 7.03 (*d*, *J* = 15.1, CH); 7.10–7.57 (*m*, 10 arom. H); 7.61 (*d*, *J* = 15.1, CH); 8.70 (br. *s*, NH, exchangeable with D_2O); 9.45 (br. *s*, NH, exchangeable with D_2O).

*Data of (*Z*)-***4b***.* ^{1}H-NMR ($CDCl_3$): 6.51 (*d*, *J* = 12.1, CH); 7.03 (br. *s*, NH, exchangeable with D_2O); 7.19 (*d*, *J* = 12.1, CH); 7.10–7.50 (*m*, 10 arom. H); 9.17 (br. *s*, NH, exchangeable with D_2O).

3. *Cell Cultures.* The cancer cell lines were obtained from *American Type Culture Collection*. Human breast cancer cell lines MDA-MB-468, and MDA-MB-231, and human colon cancer cell line SW620 were maintained in *RPMI 1640* (*Gibco/BRL*). Human colon cancer cell line HCT-116 was maintained in *McCoy's 5A* (*Gibco/BRL*). All culture media were supplemented with 10% heat-inactivated fetal bovine

serum (FBS; *Gibco/BRL*). Cell cultures were maintained at 37° under a humidified atmosphere of 5% CO_2 in an incubator.

4. *Transient Transfection and Dual-Luciferase Assays.* The STAT3 inhibitory activities of the new synthesized compounds **3**–**5** were evaluated by a modified procedure of dual-luciferase assay in human colorectal carcinoma cells HCT-116, characterized by uncontrolled expression of STAT3 [33].

Colorectal carcinoma HCT-116 cells were co-transfected with pSTAT-TA-Luc carrying firefly luciferase gene (dependently expressed by STAT3 activity), and pRL-TK carrying renilla luciferase gene (independently expressed by STAT3 activity). HCT-116 Cells were seeded at a density of 10×10^5 cells in 100 mm^2 culture plate. Beetle luciferin and coelenterazine were used as substrates for the two enzymes, resp. The cells were co-transfected with pSTAT3-TA-Luc (27 μg/plate) and internal control plasmid pRL-TK (9 μg/plate) containing the *Renilla* luciferase gene. Cells were treated with the compounds at concentration of 2 μM and incubated for 24 h. All plasmids used in this experiment were purchased from *Promega*. The transfection was carried out using *TransFectin* (*Bio-Rad*) according to the manufacturer's protocol. After 5 h of transfection, the cells were trypsinized and seeded onto sterilized black bottom 96-well plates at a density of 1×10^4 cells per well. On the following day, cells were treated with test compounds and incubated for 24 h. Firefly and *Renilla* luciferase activities were measured using dual-light reporter gene assay kit (*Promega*) on *Wallac Victor2* (*Perkin-Elmer, Inc.*, Wellesley, MA). *Renilla* luciferase activity was determined to calibrate transfection efficiency and cytotoxicity of chemicals. Relative STAT3 activity was calculated by dividing the firefly luciferase activity with *Renilla* luciferase activity in each transfection experiment.

5. *Cell Proliferation Assay.* Cells were seeded at a density of 5,000 cells per well in 96-well plates in *RPMI 1640* or *McCoy's* medium containing 10% FBS. They were replenished with fresh complete medium containing either test compound or 0.1% DMSO. After incubation for 24 or 48 h, the cell proliferation reagent *WST-1* (*Roche Applied Science*) was added to each well. *WST-1* Formazan was quantitatively measured at 450 nm with an enzyme-linked immunosorbent assay reader (*Bio-Rad*).

6. *X-Ray Crystallographic Analysis.* The crystals of **1a** and **5a** were obtained by crystallization from H_2O/MeOH 1:2 as colorless prisms, while **3a**, **10**–**11** and (*E*)-**4a** crystallized from MeOH/EtOH 1:1 soln. as transparent needles. Crystals of (*E*)-**4b** were obtained from the slow evaporation of a MeOH soln. They were mounted on an *Enraf Nonius CAD-4* diffractometer using MoK_α ($\alpha = 0.71073$ Å) radiation at 293(2) K. The lattice parameters were determined by least-squares refinements of 25 high-angle reflections. The structures were solved by direct methods [34], and the refinements were carried out by full-matrix least-squares. All non-H-atoms were refined anisotropically. The H-atoms of **1a**, **3a**, (*E*)-**4a**, and (*E*)-**4b** were detected in a difference *Fourier* synthesis and refined with isotropic thermal factors, while all H-atoms of **10**–**11** and **5a** were introduced at calculated positions, in their described geometries, and allowed to ride on the attached C-atom with fixed isotropic thermal parameters (1.2 U_{eq} of the parent C-atom). Refinements were carried out with SHELX-97 [35]. Geometrical calculations were carried out with the program PARST [36]. A summary of the crystal data, data collection, and structure refinement is presented in *Table 2*.

CCDC-739436 (**1a**), CCDC-796642, (**5a**) CCDC-758866 (**3a**), CCDC-811038 (**10**–**11**), CCDC-818273 ((*E*)-**4a**), and CCDC-846458 ((*E*)-**4b**) contain the supplementary crystallographic data for this paper (excluding structure factors). These data can be obtained free of charge *via* www.ccdc.cam.ac.uk/conts/retrieving.html (or from the *Cambridge Crystallographic Data Centre*, 12, Union Road, Cambridge CB21EZ, UK; fax: (+44)1223-336-033; or deposit@ccdc.cam.ac.uk).

Supplementary Information. Elemental analyses and ^{1}H-NMR spectra of compounds **1**–**5**, as well as crystallographic data of **1a**, **5a**, **3a**, **10**–**11**, (*E*)-**4a** and (*E*)-**4b** are available from the corresponding author.

The authors thank Prof. *Byoung-Mog Kwon,* Laboratory of Chemical Biology and Genomics, Korea Research Institute of Bioscience and Biotechnology and Department of Biomolecular Science, Korea University of Science and Technology, for the biological tests, and the University of Milano (PUR 2008) for the financial support.

Table 2. *Summary of Crystal Data and Refinement of* **1a**, **5a**, **3a**, **10**–**11**, (*E*)-**4a**, *and* (*E*)-**4b**

		1a	**5a**	**3a**	**10**–**11**	(*E*)-**4a**	(*E*)-**4b**
Empirical formula		$C_{11}H_{12}N_4O_3$	$C_{11}H_{10}N_4O_3$	$C_{11}H_{12}N_4O_2$	$C_{11}H_{12}N_4O_2$	$C_{18}H_{16}N_4O_2$	$C_{17}H_{14}N_4O_2$
Formula weight		248.25	246.23	232.20	232.25	320.35	306.33
Temp. [K]		298(2)	298(2)	298(2)	298(2)	298(2)	298(2)
MoK_α [Å]		0.71073	0.71073	0.71073	0.71073	0.71073	0.71073
Crystal system		Monoclinic	Triclinic	Monoclinic	Tetragonal	Triclinic	Triclinic
Space group		$P2_1/n$	$P\bar{1}$	$P2_1/c$	$P4_2/n$	$P\bar{1}$	$P\bar{1}$
Unit cell dimensions	a [Å]	8.139(5)	6.529(3)	13.261(5)	11.453(3)	8.706(5)	7.451(5)
	b [Å]	12.855(5)	8.797(2)	4.972(5)		8.929(5)	5.962(5)
	c [Å]	11.815(5)	9.566(6)	17.840(5)	18.499(3)	11.199(5)	16.766(7)
	α [°]		81.39(1)			87.03(1)	88.34(1)
	β [°]	109.13(1)	84.05(1)	100.58(1)		68.57(1)	80.37(1)
	γ [°]		82.65(1)			76.54(1)	93.78(1)
	V [Å^3]	1167.9(9)	536.7(4)	1156.2(9)	2426.4(9)	787.6(7)	732.1(8)
Crystal size [mm^3]		$0.49\times0.15\times0.5$	$0.4\times0.35\times0.15$	$0.5\times0.4\times0.3$	$0.45\times0.25\times0.1$	$0.8\times0.7\times0.6$	$0.5\times0.4\times0.03$
Z		4	2	4	8	2	2
Density (calc., g/cm^3])		1.412	1.524	1.334	1.272	1.351	1.390
F(000)		520	256	488	976	336	320
θ Range data coll. [°]		2.42–26.17	2.16–23.97	2.32–25.98	2.09–25.04	2.58–25.01	2.58–25.01
Index ranges		$-10\le h\le9$	$-1\le h\le7$	$-16\le h\le16$	$-13\le h\le13$	$-10\le h\le9$	$-8\le h\le8$
		$-1\le k\le15$	$-10\le k\le10$	$-6\le k\le6$	$-1\le k\le13$	$-10\le k\le10$	$-7\le k\le7$
		$-1\le l\le14$	$-10\le l\le10$	$-1\le l\le21$	$-1\le l\le21$	$-1\le l\le13$	$-19\le l\le0$
Refl. coll. (indep.)		2888/2301	2184/1687	4618/2263	5281/2143	3245/2779	2581/2581
Refinement method		Full-matrix least-squares on F^2					
Data/restraints/parameters		2301/0/151	1687/0/203	2263/0/202	2143/0/161	2779/0/281	2581/0/260
Goodness-of-fit on F^2		0.931	1.035	0.926	0.935	0.997	0.918
Final R ind. [$I>2\sigma(I)$]		$R1=0.069$	$R1=0.047$	$R1=0.043$	$R1=0.089$	$R1=0.047$	$R1=0.078$
		$wR2=0.197$	$wR2=0.117$	$wR2=0.081$	$wR2=0.193$	$wR2=0.112$	$wR2=0.219$
Largest diff. peak and hole (e [Å^3])		0.367, −0.308	0.309, −0.353	0.149, −0.167	0.325, −0.21	0.15, −0.041	0.296, −0.26

REFERENCES

[1] L. Costantino, D. Barlocco, *Curr. Med. Chem*. **2008**, *15*, 834.
[2] J. E. Darnell Jr., *Science* **1997**, *277*, 1630.
[3] H. Yu, R. Jove, *Nat. Rev. Cancer* **2004**, *4*, 97.
[4] P. C. Heinrich, I. Behrmann, G. Müller-Newen, F. Schaper, L. Graeve, *Biochem. J.* **1998**, *334*, 297.
[5] T. Hirano, K. Ishihara, M. Hibi, *Oncogene* **2000**, *19*, 2548.
[6] D. Wei, X. Le, L. Zheng, L. Wang, J. A. Frey, A. C. Gao, Z. Peng, S. Huang, H. Q. Xiong, J. L. Abbruzzese, K. Xie, *Oncogene* **2003**, *22*, 319.
[7] J. R. Grandis, S. D. Drenning, Q. Zeng, S. C. Watkins, M. F. Melhem, S. Endo, D. E. Johnson, L. Huang, Y. He, J. D. Kim, *Proc. Natl. Acad. Sci. U.S.A.* **2000**, *97*, 4227.
[8] G. Niu, T. Bowman, M. Huang, S. Shivers, D. Reintgen, A. Daud, A. Chang, A. Kraker, R. Jove, H. Yu, *Oncogene* **2002**, *21*, 7001.
[9] S. Nam, R. Buettner, J. Turkson, D. Kim, J. Q. Cheng, S. Muehlbeyer, F. Hippe, S. Vatter, K.-H. Merz, G. Eisenbrand, R. Jove, *Proc. Natl. Acad. Sci. U.S.A.* **2005**, *102*, 5998.
[10] R. Buettner, L. B. Mora, R. Jove, *Clin. Cancer Res.* **2002**, *8*, 945.
[11] M. V. Karamouzis, P. A. Kostantinipoulos, A. G. Papavassiliou, *J. Mol. Med.* **2007**, *85*, 427.
[12] G. Niu, K. H. Shain, M. Huang, R. Ravi, A. Bedi, W. S. Dalton, R. Jove, H. Yu, *Cancer Res.* **2001**, *61*, 3276.
[13] J. Turkson, D. Ryan, J. S. Kim, Y. Zhang, Z. Chen, E. Haura, A. Laudano, S. Sebti, A. D. Hamilton, R. Jove, *J. Biol. Chem*. **2001**, *276*, 45443.
[14] D. Masciocchi, A. Gelain, S. Villa, F. Meneghetti, D. Barlocco, *Future Med. Chem.* **2011**, *3*, 567.
[15] B. M. Kwon, D. C. Han, K. H. Son, D. S. Shin, J. Lee, US Pat. 2008/00514442 A1, 2008.
[16] D.-S. Shin, D. Masciocchi, A. Gelain, S. Villa, D. Barlocco, F. Meneghetti, A. Pedretti, Y.-M. Han, D. C. Han, B.-M. Kwon, L. Legnani, L. Toma, *Med. Chem. Commun.* **2010**, *1*, 156.
[17] S. Marumoto, H. Kogen, S. Naruto, *J. Org. Chem.* **1998**, *63*, 2068.
[18] T. Granier, A. Vasella, *Helv. Chim. Acta* **1998**, *81*, 865.
[19] J. D. White, P. Hrnciar, *J. Org. Chem.* **2000**, *65*, 2646.
[20] A. Consonni, B. Danieli, G. Lesma, D. Passarella, P. Piacenti, A. Silvani, *Eur. J. Org. Chem.* **2001**, 1377.
[21] A. Schrey, F. Osterkamp, A. Straudi, C. Rickert, H. Wagner, U. Koert, B. Herrschaft, K. Harms, *Eur. J. Org. Chem.* **1999**, 2977.
[22] V.-D. Le, C.-H. Wong, *J. Org. Chem.* **2000**, *65*, 2399.
[23] C. Yu, L. Hu, *Tetrahedron Lett.* **2001**, *42*, 5167.
[24] J. L. Jiménez Blanco, C. Saitz Barría, J. M. Benito, C. Ortiz Mellet, J. Fuentes, F. Santoyo-Gonzáez, J. M. García Fernández, *Synthesis* **1999**, *11*, 1907.
[25] X. Chungu, Faming Zhuanli Shenquing Gongkai Shoumingshu, CN1966491, 2007.
[26] A. G. M. Barrett, D. Hamprecht, M. Ohkubo, *J. Org. Chem*. **1997**, *62*, 9376.
[27] L. J. Farrugia, *J. Appl. Crystallogr*. **1999**, *32*, 837.
[28] D. Cremer, J. A. Pople, *J. Am. Chem. Soc*. **1975**, *97*, 1354.
[29] T. L. Kurth, F. D. Lewis, *J. Am. Chem. Soc*. **2003**, *125*, 13760.
[30] X. Zhao, Y. L. Chang, F. W. Fowler, J. W. Lauher, *J. Am. Chem. Soc*. **1990**, *112*, 6627.
[31] P. Metrangolo, H. Neukirch, T. Pilati, G. Resnati, *Acc. Chem. Res.* **2005**, *38*, 386.
[32] A. B. Sheremetev, Y. L. Shamshina, D. E. Dmitriev, *Russ. Chem. Bull*. **2005**, *54*, 1032.
[33] B. A. Sherf, S. L. Navarro, R. R. Hannah, K. V. Wood, *Promega Notes* **1996**, *57*, 2.
[34] A. Altomare, G. Cascarano, C. Giacovazzo, A. Guagliardi, G. Polidori, M. C. Burla, M. Camalli, *J. Appl. Crystallogr.* **1994**, *27*, 435.
[35] G. M. Sheldrick, SHELX-97, Program for the Refinement of Crystal Structure, University of Göttingen, Germany, 1997.
[36] M. Nardelli, *J. Appl. Crystallogr.* **1995**, *28*, 659.

Received October 19, 2011